



OPEN 'Candidatus liberibacter solanacearum' protein CKC_05770 interacts in vivo with tomato APX6 and APX7

Julien Gad Levy^{1,2,4}✉, Adwaita Prasad Parida^{1,4}, Junepyo Oh^{1,4}, Azucena Mendoza-Herrera¹, Brian D. Shaw³ & Cecilia Tamborindeguy¹✉

Pathogens have evolved mechanisms to manipulate their hosts to facilitate effective colonization and infection. One such mechanism involves the secretion of effectors that interfere with the host immune response. Effectors are typically secreted by dedicated secretion machinery that delivers the protein to the host cell. Liberibacters are intracellular bacterial pathogens that do not encode the typical secretion systems employed to secrete effectors; therefore, other mechanisms might be at play to allow Liberibacters to infect their hosts, such as the secretion of effectors via the sec-secretion system or via non-classical secretion systems. In this study, we datamined the genomes of five Liberibacter pathogens and identified from 66 to 102 putative non-classical secreted proteins encoded. Then, we focused on two predicted non-classical secreted proteins encoded by 'Candidatus Liberibacter solanacearum' haplotype B, CKC_05770 and CKC_00930, which showed similarities to non-classical secreted effectors from other *Liberibacter* species. We evaluated their secretion using alkaline phosphatase assays, if they suppressed programmed cell death or reactive oxygen species accumulation in *Nicotiana benthamiana* upon transient expression, and whether they could interact with tomato ascorbate peroxidases. We also evaluated if CKC_05770 had a peroxidase activity. Our results suggest that CKC_05770 interacted with tomato ascorbate peroxidases in two in vivo assays but not in vitro. Further, CKC_05770 did not suppress plant immunity nor did it have a peroxidase activity as the 'Candidatus Liberibacter asiaticus' homologs did. Therefore, Liberibacter pathogens encode non-classical secreted proteins that could be effectors, but the roles of these proteins need to be validated in each pathosystem.

Keywords Candidatus liberibacter asiaticus, Citrus, ROS, Huanglongbing, Hypersensitive response

Liberibacters are devastating pathogens of many economically important crops. They are gram-negative phloem-limited alpha-proteobacteria transmitted by psyllids. Among them, 'Candidatus Liberibacter solanacearum' (Lso) infects different plant families. While at least ten Lso haplotypes have been identified and are denominated with different letters (A, B, C, etc, hereafter refer to as LsoA, LsoB, LsoC, etc.)^{1–7}. LsoA and LsoB haplotypes infect solanaceous plants in the United States causing zebra chip in potato plants and permanente del tomato (vein-greening) in tomato plants. LsoA and LsoB are transmitted by the tomato psyllid, *Bactericera cockerelli* Šulc (Hemiptera: Trioizidae), also known as the potato psyllid^{8–10}. LsoC, LsoD and LsoE infect carrot plants and other apiaceous crops; LsoC is found in northern Europe where *Trioza apicalis* transmits it while LsoD and LsoE are found in the Mediterranean basin and are transmitted by *B. trionica*^{4,11–14}. Other species of Liberibacter pathogens exist, for example, 'Candidatus Liberibacter asiaticus' (CLas) infects citrus in different parts of the world and is transmitted by *Diaphorina citri*¹⁵.

In an effort to understand the molecular mechanisms involved in Liberibacter pathogenicity, a large body of literature has focused on Lso and CLas effectors. Effectors are proteins secreted by the pathogen into the eukaryotic host where they have different effects such as immunity disruption or favoring host colonization¹⁶. Liberibacter pathogens lack the secretion systems commonly used by gram-negative bacterial pathogens to

¹Department of Entomology, Texas A&M University, College Station, TX 77843, USA. ²Department of Horticultural Sciences, Texas A&M University, College Station, TX 77843, USA. ³Department of Plant Pathology and Microbiology, Texas A&M University, College Station, TX 77843, USA. ⁴These authors contributed equally: Julien G. Levy, Adwaita Parida and Junepyo Oh. ✉email: julienlevy@tamu.edu; ctamborindeguy@tamu.edu

secrete effectors^{17,18}. However, because these bacteria are intracellular pathogens, effectors could be secreted by the type I secretion system (T1SS) and the Sec-dependent secretory machinery. Several candidate effectors secreted by these systems have been identified, some examples are in the following literature^{19–28}.

Despite the large body of studies dedicated to protein secretion by bacteria, not all mechanisms have been identified yet. For instance, several bacterial proteins lacking the typical secretion domains are secreted²⁹. *Liberibacter* proteins secreted via non-classical secretory systems could also be effectors playing a key role in bacterial pathogenicity. Indeed, non-classical secreted effector proteins have been identified in CLas^{20,30,31}, but not in Lso.

In the present study, we tested if two Lso encoded non-classical secreted proteins could manipulate the host immune responses or interact with host proteins. First, we datamined the genome of the five *Liberibacter* pathogens (LsoA, LsoB, LsoC, LsoD and CLas) and the culturable *Liberibacter crescens* to identify putative non-classical secreted proteins. Then, we focused on two of these proteins encoded in the LsoB genome, CKC_00930 and CKC_05770. These proteins were selected because a CLas homolog (AGH17488) was already characterized; this protein interacts with the plant ASCORBATE PEROXIDASE6 (APX6) and inhibits reactive oxygen species (ROS) accumulation and lipid oxidation³¹. The two Lso proteins are also similar to two other CLas secreted proteins, SC1_gp095 and SC2_gp095, the latter is a functional peroxidase³⁰. Further, while LsoA encoded two genes with high similarity to CKC_05770, LsoB appears to encode CKC_05770 and a truncated version, CKC_00930, described in detail below. Therefore, these genes could be linked to the difference in pathogenicity reported between LsoA and LsoB^{32–34}. To evaluate if these two Lso proteins could be effectors, we evaluated their secretion using *Escherichia coli* as a surrogate system. Then, we performed bioassays to determine if the identified proteins could disrupt plant immunity. Finally, we tested if these proteins were able to interact with tomato ascorbate peroxidase proteins.

Results

Identification of putative non-classically secreted proteins

The bioinformatic analyses identified between 66 and 102 putative non-classical secreted proteins in the *Liberibacter* pathogen genomes and 69 in *L. crescens* (Table 1 and Table S2). These proteins had a SecretomeP score greater than 0.7 and were not identified as encoding a signal peptide by SignalP 6.0.

Bioinformatic analyses of CKC_05770 and CKC_00930

Among the SecretomeP identified proteins were LsoB CKC_05770 (SecP score of 0.948575) and CKC_00930 (SecP score of 0.914758). Both proteins were predicted by SignalP6.0 as not secreted using any of the classical bacterial secretion systems (Other score > 1).

CKC_05770 encodes a hypothetical protein that is 234 amino acids long. CKC_00930 encodes a 60-amino acid-long hypothetical protein that is 100% identical to the last 60 amino acids in the C-terminal region of CKC_05770. CKC_05770 and CKC_00930 are within each of the two LsoB prophage-like regions. Prophage 1 is located between the nucleotides 180,904 and 194,624 of the published LsoB genome sequence (GenBank ID CP002371.1) and contains the predicted genes CKC_00890 to CKC_00950. Prophage 2 is located between the nucleotides 1,218,755 to 1,232,772 and contains the predicted genes CKC_05730 to CKC_05790 (Fig. 1A shows a diagram of the genomic regions surrounding CKC_00930 and CKC_05770).

A BLASTP search identified two genes with a high degree of similarity to CKC_05770 in the genomes of Lso haplotypes A (strains New Zealand and RSTM) and C. These genes encoded proteins of approximately 234 amino acids long. To verify if the shorter CKC_00930 protein was not the result of a gene prediction error, we performed a TBLASTN search using the sequence of CKC_05770 as a query against the Lso haplotype B genome. An additional hit with a high level of similarity to the N-terminal half of CKC_05770 was identified between the predicted genes CKC_00935 and CKC_00940 and was labeled as CKC_00931 in Fig. 1A. In silico translation of this region yielded a putative 241-amino acid long protein, of which the first 174 amino acids showed similarity to CKC_05770. Amplification of CKC_00931 using specific primers (931 F and 931R) failed; similarly, attempts to validate the existence of CKC_00930; e.g. using primers 930R and 935R, also failed. Several primers were designed to amplify the region and were used in different combinations. We successfully amplified two amplicons of different sizes with primers 925R and 930R (Fig. 1B). The longest fragment was 759 nucleotides long and corresponded to the Lso prophage 2 sequence, it included CKC_05770 and the end of CKC_05775. The shorter fragment was 440 nucleotides long and contained a portion of CKC_00925, a portion of CKC_00931, and CKC_00930. Based on these results, we concluded that this region of prophage 1 had a different rearrangement in our laboratory strain (Fig. 1B, primer 925R also matches CKC_05775 and CKC_00935).

Genome (strain, assembly)	Number of putative non-classical secreted proteins identified
Lso haplotype A (LsoNZ, ASM96808v1)	102
Lso haplotype B (CLso-ZC1, ASM18366v1)	75
Lso haplotype C (FIN114, ASM198367v1)	85
Lso haplotype D (ISR100, ASM291824v2)	77
CLas (psy62, ASM2376v2)	66
<i>L. crescens</i> (BT-0, ASM154330v1)	69

Table 1. Summary of the non-classical secreted proteins identification in liberibacter genomes.

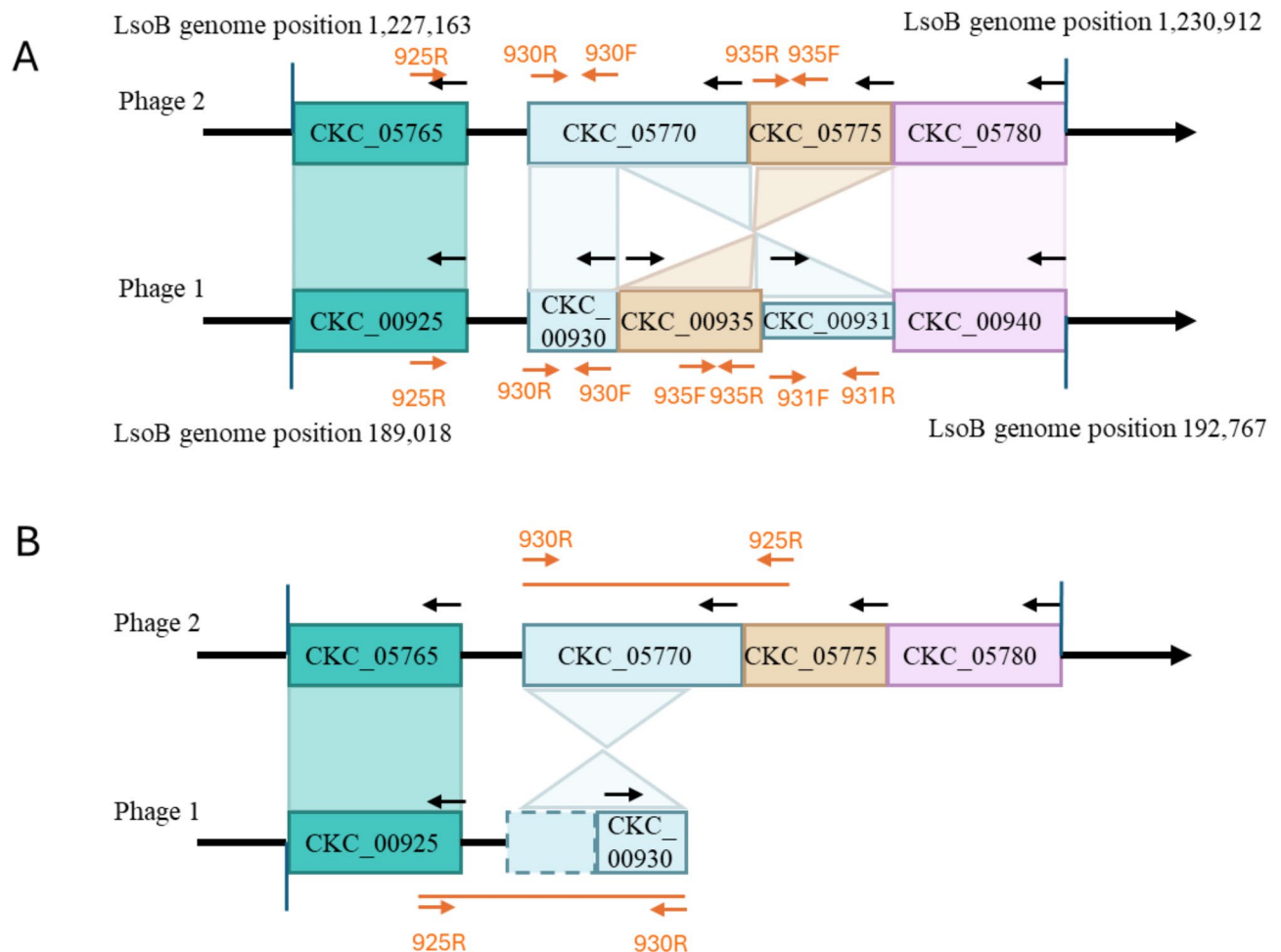


Fig. 1. Schematic diagram of the two phage regions containing the genes CKC_05770 and CKC_00930. Each colored box represents a gene (the length of the genes is not at scale), with genes of the same color representing homolog genes. **A:** Phage regions based on the published genome. The putative CKC_00931 gene is represented by a box of smaller height. These regions are highly similar: 100% similarity for the region including CKC_00925 and CKC_0930 (1237 nucleotides), 100% similarity between CKC_00935 and CKC_05775, and 99% similarity between CKC_00940 and CKC_05780 (1649 out of 1668 nucleotides). CKC_931 shared 90% similarity with the N-terminal half of CKC_05770 (486 out of 540 nucleotides). **B:** Phage regions in the LsoB strain in our laboratory. The black arrows represent whether the genes are encoded in the sense or anti-sense strand. The orange arrows in A represent the different primers designed to validate the existence of CKC_00930 and CKC_00931, 931 F targets phage 1 only. In B, the orange arrows represent where the primers that allowed us to sequence CKC_00930 in our laboratory strain primed. The orange lines represent the sequenced amplicons used to identify the rearrangement of Phage 1 in our laboratory strain. The dashed box represents the partial sequence identical to CKC_05770 but probably not encoding a protein.

We also identified one or two homolog genes in different CLas genomes while only one gene was identified in the ‘*Ca. L. africanus*’ (CLaf), ‘*Ca. L. americanus*’ (CLam) and ‘*Ca. L. europaeus*’ (CLEu) genomes. No homologs were found in *L. crescens* or in Lso haplotype D.

A phylogenetic tree was constructed with the identified proteins. Only the genes from the CLas strains gpxsy, psy62, UF506 and A4 were used for the tree (Fig. 2). Lso proteins clustered together in the tree, and among those, the proteins encoded by the Lso genomes associated with tomato psyllids and solanaceous crops (LsoA and LsoB) showed a higher degree of similarity among themselves. The Lso proteins shared between 59 and 100% of identity. The proteins encoded by the pathogens causing huanglongbing (CLas, CLam, and CLaf) did not cluster together: CLas proteins formed a cluster with high degree of similarity to Lso proteins, while the CLaf and CLam proteins clustered in a different clade with the CLEu protein (Fig. 2).

Overall, these proteins did not share a high degree of similarity among different species. For example, the CLas protein WP_015825009.1 (SC2_gp095) shared less than 30% identity with CKC_05770.

All the identified genes are annotated as hypothetical proteins and were predicted to encode non-classical secreted proteins. Searches with Interproscan for specific domains only identified disordered domains in each protein.

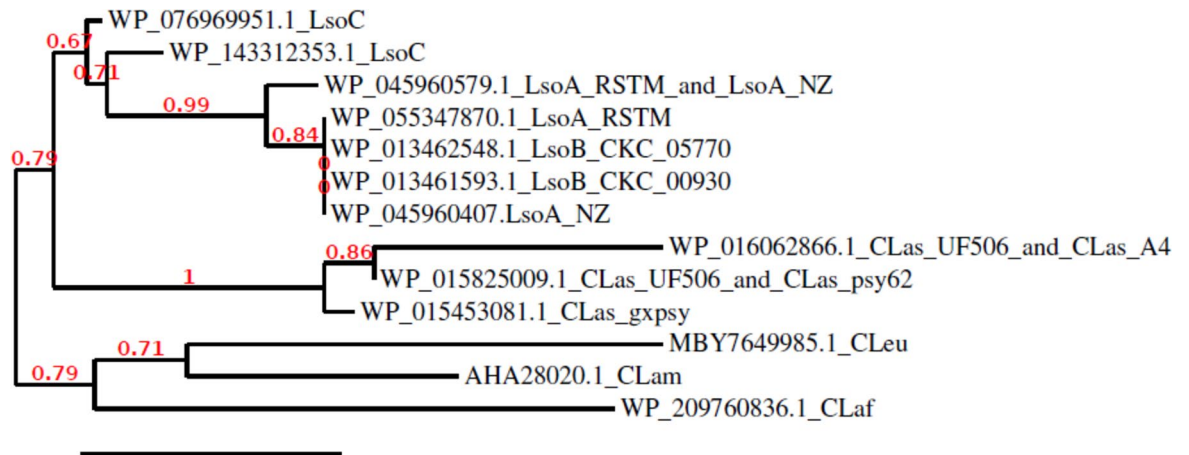


Fig. 2. Phylogenetic analysis of Liberibacter proteins homologous to Lso CKC_00930 (WP_013461593.1) and CKC_05770 (WP_013462548.1). Of note, WP_015453081.1 is AGH17488, and WP_015825009.1 and WP_016062866.1 are SC1_gp095 and SC2_gp095, respectively. The scale bar indicates the branch length. The protein accession numbers are given in the figure.

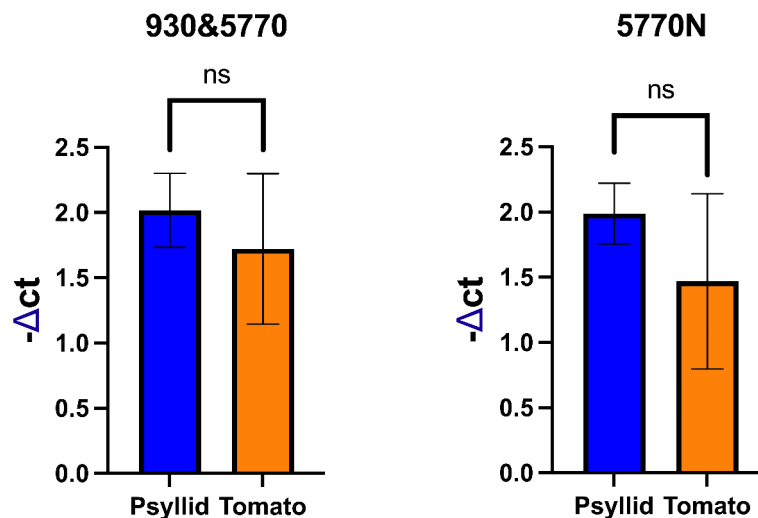


Fig. 3. Relative expression of the candidate genes in LsoB-infected tomato plants and psyllids. Gene expression was quantified using RT-q PCR and analyzed using the ΔC_t method. Two primer sets were used, one amplifying exclusively CKC_05770 (CKC_05770N) and one amplifying a common CKC_05770 and CKC_00930 region (930&5770). The expression level was normalized relative to Lso RecA gene. Bars represent mean $\Delta C_t \pm$ standard error of the mean ($n = 3$). No significant differences were observed (p -value > 0.05 , ns).

Expression analysis and copy number

We evaluated the expression of the candidate genes by RT-qPCR in psyllids and tomato plants infected with LsoB. Because CKC_00930 is identical to the C-terminal domain of CKC_05770, two sets of primers were designed, one amplifying the common region (5770&930) and one specific to the N-terminal portion of CKC_05770 (CKC_05770N). The results indicated that CKC_05770 was expressed in LsoB-infected psyllids and tomato plants (Fig. 3). Similar gene expression profiles were observed with both primer sets: no significant differences in expression were observed when comparing infected tomato plants and psyllids.

Because differences in the copy number of bacteriophage genes were identified in CLas associated with different hosts³⁵, we also evaluated the copy number of the candidate genes when LsoB was associated with psyllids and tomato plants. Gene copy number was calculated using LsoB RecA as a reference. Similar copy numbers were identified with each primer pair between insects and tomato plants (Fig. 4). A copy number of around 1 was obtained with the CKC_05770N primers and of around 5 with the primers targeting CKC_00930 and CKC_05770; this higher number is probably due to the primers targeting two genes in the genome.

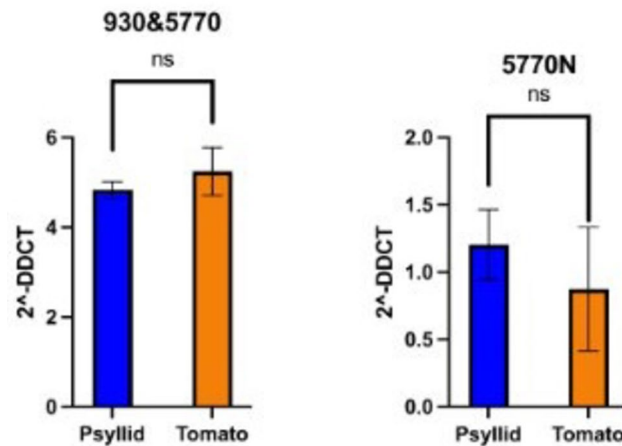


Fig. 4. Relative gene quantification of CKC_05770 (CKC_05770N) and of the common CKC_05770 and CKC_0930 region in plants and insects. The copy number was normalized relative to the chromosomal Lso RecA gene. Bars represent $2^{-\Delta\Delta C_t} \pm$ standard error of the mean ($n=3$). No significant differences were observed ($p\text{-value} > 0.05$, ns).

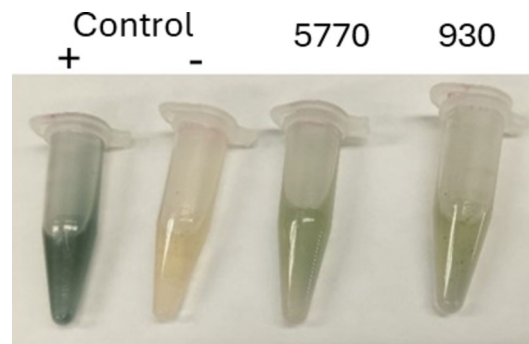


Fig. 5. Alkaline phosphatase (PhoA) assay for protein secretion from filtered supernatant. CKC_05770 and CKC_0930 were cloned in fusion with a *PhoA* reporter gene. The light blue coloration in the candidate's supernatant validates the SecretomeP prediction.

Secretion validation

An alkaline phosphatase (*phoA*) gene fusion test was used to evaluate the secretion of CKC_0930 and CKC_05770 by *E. coli*. While *E. coli* cells with an empty pJDT1-SDM vector remained white in the presence of 5-bromo-4-chloro-3-indolyl phosphate (5-BCIP), bacteria with the fusion CKC_05770-*phoA* and CKC_0930-*phoA* turned blue. We further evaluated the secretion by testing the phosphatase activity of the filtered bacterial culture supernatant. The filtered media from both bacterial cultures turned blue while the negative control remained white (Fig. 5). These results suggest that both proteins can be secreted by bacteria into the surrounding medium.

Suppression of plant cell death and ROS accumulation

Transient expression of CKC_05770 or CKC_0930 did not induce cell death in *Nicotiana benthamiana* (not shown). To evaluate if the candidate effectors could suppress plant cell death, they were co-infiltrated with Prf^{D1416V}, a cell death inducer. Cell death scores following co-infiltration of the candidate effectors CKC_05770 or CKC_0930 with Prf^{D1416V} averaged 5.3 and 6.1, respectively. These scores were not significantly different ($p\text{-value} > 0.05$) than the scores obtained for the transient expression of Prf^{D1416V} co-infiltrated with empty vector, the positive control for cell death (average score 5.5). The co-infiltrations of Prf^{D1416V} with AvrPto1 used as a control for the suppression of cell death resulted in significantly lower cell death scores (average score 1.6) (Fig. 6A).

Co-infiltrations with BAX were also tested. Bax is another protein causing cell death when expressed in *N. benthamiana*³⁶. Cell death scores following co-infiltration of the candidate effectors with BAX (average score 6.63 for both effectors) were not significantly different ($p\text{-value} > 0.05$) than the scores obtained for the transient expression of BAX co-infiltrated with empty vector (average score: 7.15, Fig. 6B).

We evaluated if the candidate proteins could suppress ROS bursts. Transient expression of CKC_05770 or CKC_0930 did not affect ROS accumulation in *N. benthamiana* leaves compared to controls agroinfiltrated with the empty vector ($p\text{-value} > 0.05$) (Fig. 7).

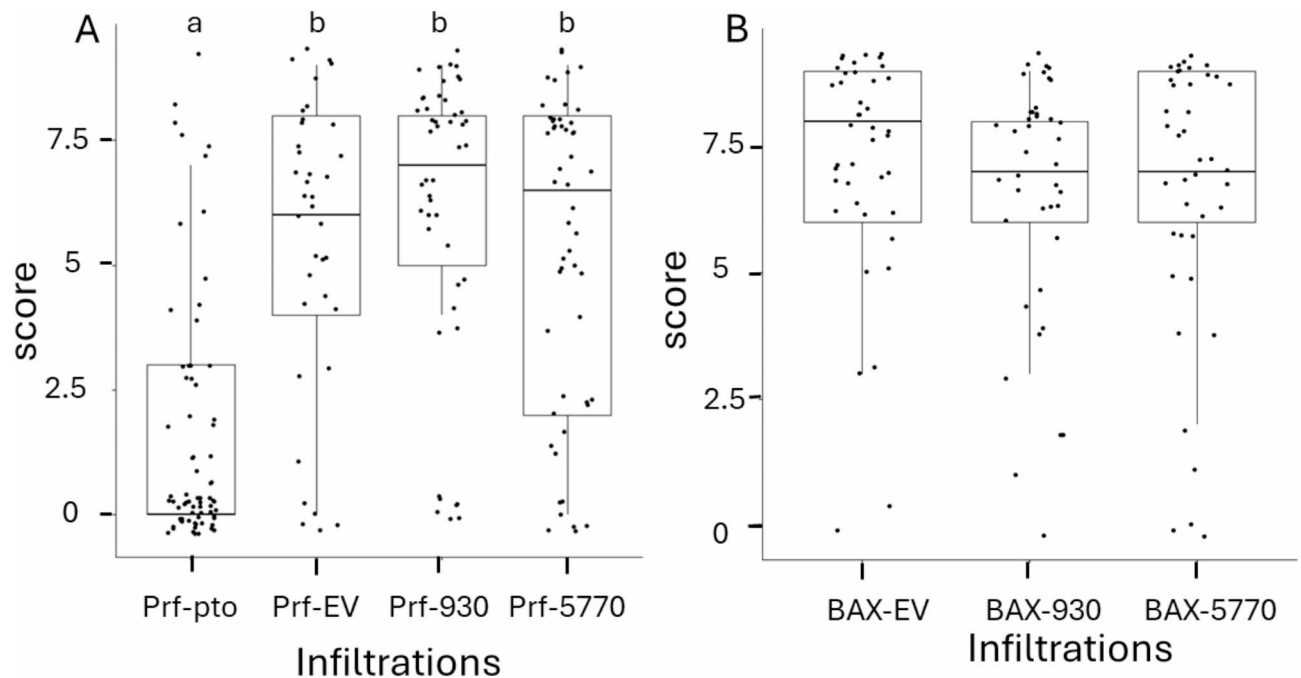


Fig. 6. Cell death suppression assays. Cell death was scored 7 days after infiltration of *N. benthamiana* leaves. **(A)** Co-infiltration with Prf^{D1416V} and each candidate, CKC_930 (Prf-930) and CKC_5770 (Prf-5770), with the controls empty vector (Prf-EV), or with AvrPto1 (Prf-pto). **(B)** Similar experiments were conducted using BAX as cell death inducer. Cell death was scored on a scale of 0 to 10. Letters represent significant differences for each effector using Kruskal-Wallis (p -value < 0.05) and Wilcoxon post-hoc tests.

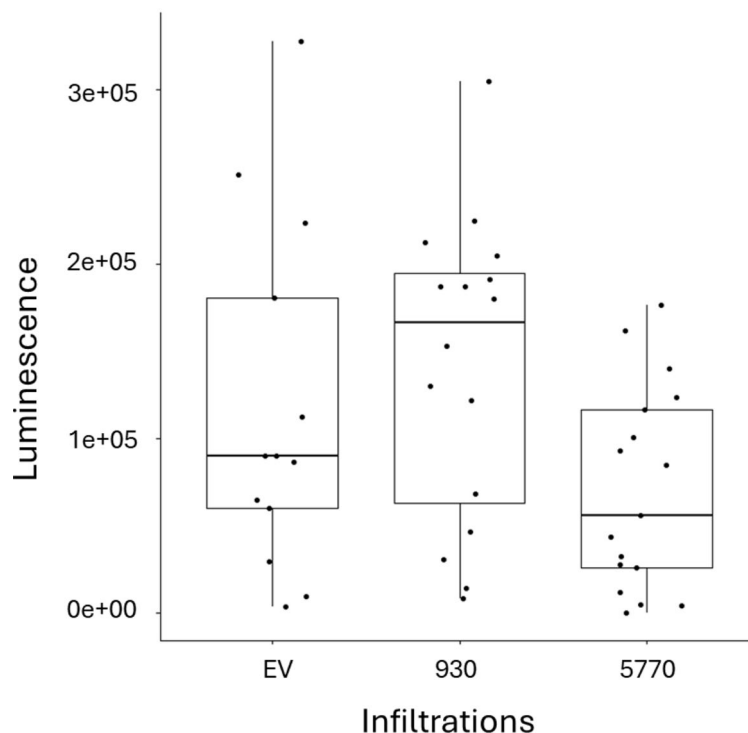


Fig. 7. Reactive oxygen species assays. pEG101 (EV, empty vector control), CKC_05770 and CKC_00930 were transiently expressed in *N. benthamiana* following *A. tumefaciens* infiltration. Leaf disks were taken 24 h post infiltration, and ROS was quantified after challenged with 1 μ M flg22.

Yeast-two-hybrid interaction between LsoB CKC_05770 and CKC_00930 and tomato APX1, APX6, and APX7

Since AGH17488, the CLas homolog, interacts with a citrus and tobacco chloroplastic ascorbate peroxidase APX6³⁷, we evaluated the interaction of LsoB CKC_05770 and CKC_00930 with the two tomato chloroplastic ascorbate peroxidases, APX6 and APX7, by yeast-two hybrid assays (Fig. 8). Based on the yeast two-hybrid results, CKC_05770 interacted with tomato APX6 and APX7. CKC_00930 autoactivated the yeast two-hybrid system, therefore we could not test the interaction of this protein with the tomato ascorbate peroxidases (Fig. S2).

CKC_00930 is identical to the last 60 AA in the C-terminal end of CKC_05770, thus, we also evaluated the interaction of the 105 AA in the N-terminal portion of CKC_05770 (CKC_05770N) with tomato APX6 and APX7. CKC_05770N did not interact with tomato APX6 or APX7 based on Y2H assays (Fig. S2).

We also evaluated whether CKC_05770 or CKC_05770N interacted with APX1, one of the three tomato cytoplasmic APX proteins. Based on yeast-two hybrid results, tomato APX1 did not interact with CKC_05770 or CKC_05770N (Fig. 8 and Fig. S2).

As controls of the yeast two-hybrid assays, we verified that yeast did not grow in the selective QDO medium when yeasts were transformed with the tomato APX proteins and the empty pDEST-GKBT7 vector or when they were transformed with CKC_05770, CKC_05770N and the empty pDEST-GADT7 vector (not shown).

Bimolecular fluorescence complementation

The interactions between CKC_05770 and CKC_00930 with tomato APX6 and APX7 proteins were also evaluated using BiFC. Fluorescence was observed in the cell cytoplasm when CKC_05770 fused to the C-YFP was co-expressed with tomato APX6 or APX7 fused to the N-YFP (Fig. 9). No signal was observed when the proteins were co-expressed in the control experiments. These results suggest that these proteins can interact in vivo validating the Y2H assay results. Furthermore, the interaction was observed in the cytoplasm, and it did not overlap with the chlorophyll signal, therefore, the interaction did not occur in the chloroplasts. No signal was observed when we evaluated the interaction between CKC_00930 and APX6, or APX7 (not shown).

The subcellular localizations of CKC_05770 and CKC_00930 were evaluated by transiently expressing each protein fused to a yellow fluorescent protein (YFP) in *N. benthamiana* leaves. Both proteins were observed in the cytoplasm and some nuclei of the *N. benthamiana* epidermal cells (Fig S3, File S1). Therefore, while CKC_05770 has a nucleus-cytoplasmic localization, the interaction with APX6 and APX7 occurs in the cytoplasm only.

Pull-down assay

The interaction between CKC_05770 and tomato APX7 was also evaluated by pull-down assays. The interaction between these proteins could not be validated using this in vitro approach (Fig S4).

Peroxidase assay

Because of the similarity between CKC_05770 and the functional peroxidase protein CLas SC2_gp095³⁰, we tested if CKC_05770 had a peroxidase function. The populations of *E. coli* treated with H₂O₂ stopped growing even when the expression of CKC_05770 was induced. The untreated populations (controls) continued to grow (Fig. 10). These results suggest that CKC_05770 did not have a peroxidase activity.

Discussion

Pathogens have evolved numerous secreted proteins, effectors, that inhibit host defenses and promote infection by modifying host components. Pathogenic bacteria usually have specific secretion systems for these effector proteins. However, *Liberibacter* pathogens lack the typical secretion systems employed by bacterial pathogens to secrete effectors, but because these bacteria are intracellular pathogens, proteins secreted via the Sec-dependent secretion system or via other mechanisms can act as effectors. Through datamining the genomes of five *Liberibacter* pathogens we have predicted between 66 and 102 non-classical secreted candidate proteins per genome. Sixty-nine putative non-classical secreted proteins were predicted in the genome of *L. crescens*, a

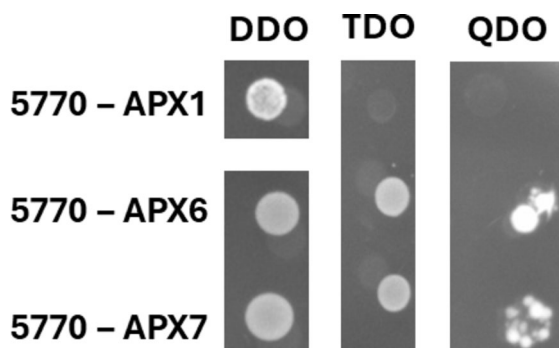


Fig. 8. Yeast two-hybrid assay between CKC_05770 and tomato APX1, APX6 and APX7. Yeasts transformed with each plasmid combination grew in the non-selective DDO medium, only yeasts carrying CKC_05770 and tomato APX6 or APX7 grew in the selective media TDO and QDO.

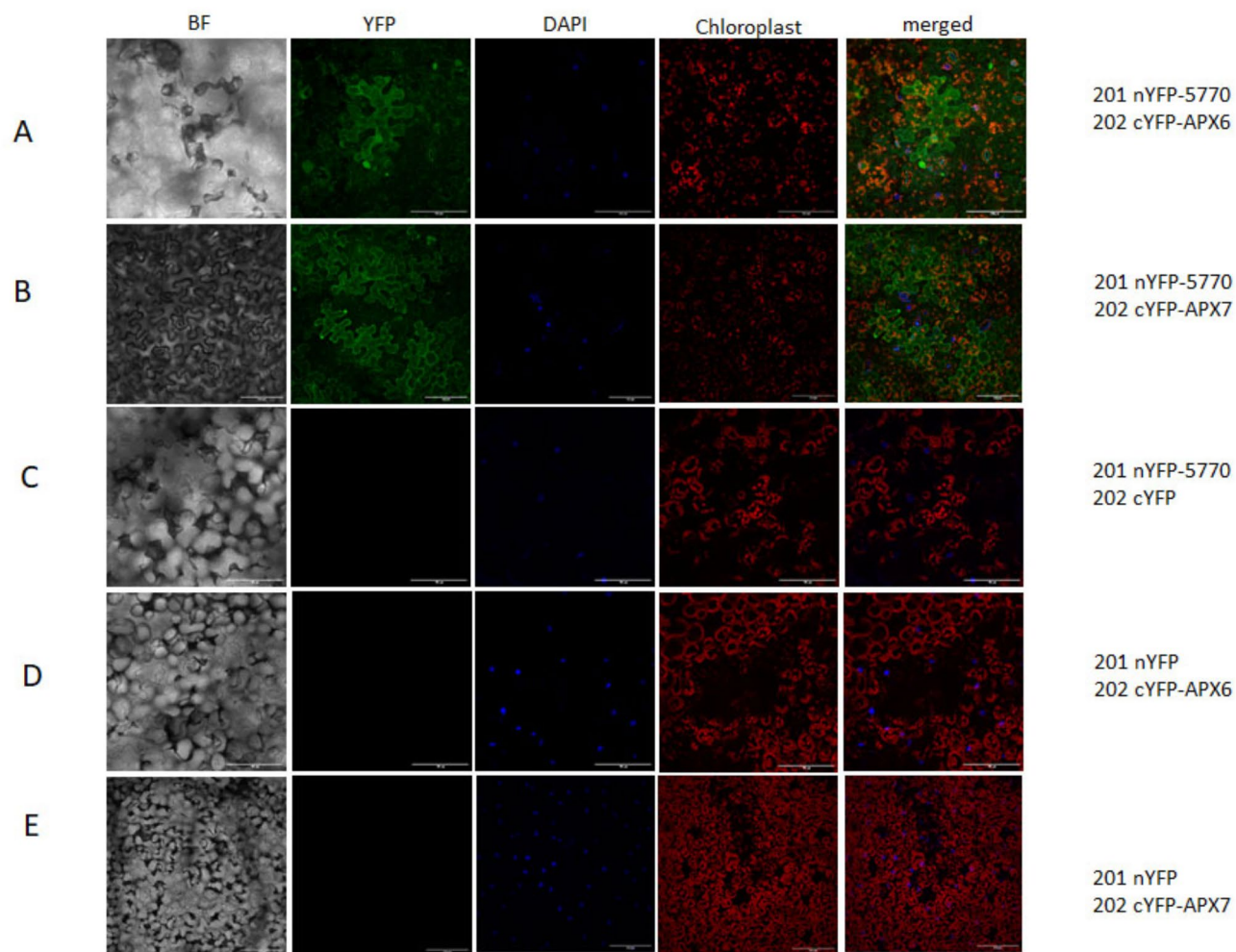


Fig. 9. Bi-molecule fluorescence complementation (BiFC) analysis of CKC_5770 interaction with tomato APX6 and APX7. *N. benthamiana* leaves were infiltrated with a 1:1 ratio of agrobacteria containing CKC_5770-YC and APX6-YN (A) or APX7-YN (B). Images were taken 3 days post-infiltration. Co-infiltrations of CKC_5770-YC with empty YN vector (C), and empty YC vector with tomato APX-YN were performed as negative control (D and E). Scale bar represents 100 μ m.

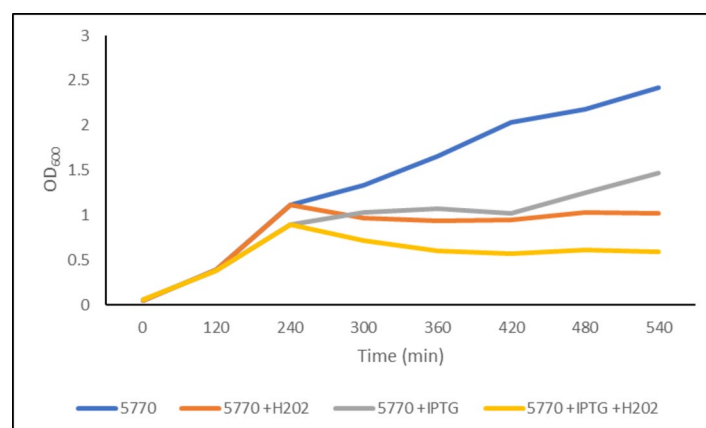


Fig. 10. CKC_05770 did not protect *Escherichia coli* against H_2O_2 . *Escherichia coli* population growth in liquid culture was evaluated by measuring the OD_{600} . Bacteria carried CKC_05770 cloned in pET101. CKC_05770 expression was induced in two of the four subcultures by adding IPTG at 120 min; two hours later (240 min) one induced and one non-induced subculture were treated with 3% H_2O_2 .

culturable *Liberibacter*. The variation on the number of putative non-classical secreted proteins could result from differences in gene content among genomes and from differences in the prediction parameters used for each genome. Indeed, some predicted non-classical secreted proteins such as flagellin (LsoB ADR52278.1) were identified in several *Liberibacter* genomes, while other candidate proteins were found in only one genome, e.g. LsoB ADR52325.1 encoding a hypothetical protein CKC_02880.

We chose to evaluate the predicted LsoB CKC_00930 and CKC_05770 proteins because homologs of these proteins were identified in the *Liberibacter* pathogens (with the exception of LsoD), but no homologs were identified in the culturable bacterium *L. crescens*. Further, CLas homologs were determined to have peroxidase activity³⁰ and interact with citrus and tobacco APX6, a chloroplastic ascorbate peroxidase³⁷. Finally, while the other Lso haplotypes encoded two homologs, LsoB encoded only one homolog, CKC_05770, and a shorter protein, CKC_00930, which was identical to the C-terminal region of CKC_05770.

PhoA tests confirmed that the full-length CKC_05770 and CKC_00930 proteins were secreted when expressed in *E. coli* in fusion with the phoA reporter gene. By quantifying the prophage genes and their expressions using the specific primers CKC_5770N (prophage 2), the common primers CKC_5770&930 (prophages 1 and 2) and using the chromosomal RecA gene as a reference (1 copy), we determined similar copy number and expression level of the prophages in Lso-infected tomato plants, and tomato psyllids. Previous study with CLas in citrus, periwinkle and psyllids determined that stress such as temperature or antibiotic treatment as well as interaction with a specific host induced an increase in phage copy which is evidence of lysogenic to lytic conversion^{38–40}. Based on our results, we did not observe lytic conversion for LsoB between the tomato host and psyllid vector. Also, the CLas homolog was expressed at higher level in plants than insects³⁰, but no differences were observed in current study.

The transient expression of CKC_05770 and CKC_00930 in *N. benthamiana* leaves was used to investigate their role in plant immunity. In single infiltration assay, neither the CKC_05770 nor CKC_00930 protein generated visible cell death. In co-infiltration assays, the proteins could not suppress cell death induced by Pr^{FD1416V} or by BAX. The CLas homolog AGH17488.1 from the gxpsy strain was found to suppress BAX-induced cell death³¹.

We also found that neither CKC_05770 nor CKC_00930 were able to reduce ROS accumulation. ROS burst is a marker of plant HR, and is one of the first responses to pathogen infection and to insect infestation^{41,42}.

Because CLas SC2_gp095³⁰, a CLas homolog, is a functional peroxidase, we evaluated if CKC_05770 had a similar function. Expression of this protein could not protect *E. coli* cells against H₂O₂. These results could explain why CKC_05770 did not reduce ROS accumulation. The CLas and Lso proteins share little similarities (less than 30% identity) therefore it is not surprising they might have different roles during the plant infection. Based on our results, these proteins encoded by different *Liberibacter* pathogens might play different roles during plant infection which might explain some of the physiological differences between the diseases they cause.

Since the functions of these proteins appear to be different, we evaluated if CKC_05770 and CKC_00930 interacted with tomato APX6 as previously shown for AGH17488. We also evaluated the interaction with APX7, the other tomato chloroplastic APX protein, and with APX1, one tomato cytoplasmic APX protein. CKC_05770 interacted with APX6 and APX7 but not with APX1 in yeast two-hybrid and BiFC experiments. Since CKC_00930 is identical to the C-terminal half of CKC_05770, we tested if both halves of CKC_05770 interacted with the APX proteins. The N-terminal part of CKC_05770 did not interact with the APX proteins tested. We were not able to evaluate the interactions for CKC_00930 interactions (CKC_05770_C terminal part) with the tomato APX proteins by yeast two-hybrid because this candidate autoactivated the system. However, we did not detect an interaction between CKC_00930 with APX6 or APX7 in the BiFC assays. We also evaluated if CKC_05770 could interact in vitro with APX7 using pull-down assays but we failed to verify the interaction. Based on these results, we concluded that if CKC_05770 and APX6 or APX7 interact, the interaction involved the complete CKC_05770 protein, and not just the N- or the C-terminal domain.

Ascorbate peroxidase (APX) is a H₂O₂-scavenging enzyme and is indispensable for the protection of chloroplasts and other cell constituents from damage by H₂O₂⁴³. A number of studies have succeeded in improving plant abiotic stress resistance by stabilizing the APX enzymes⁴⁴. Further, Durner and Klessig⁴⁵ showed that salicylic acid inhibited APX activity which correlated with the induction of defense-related genes in tobacco and enhanced resistance to tobacco mosaic virus. Therefore, APX proteins may be good targets to improve plant defense against *Liberibacter* pathogens^{37,46} as suggested by the interaction of these *Liberibacter* proteins with APX6 and/or APX7. In the case of CLas, the interaction could promote the APX enzyme activity which would inhibit HR and facilitate bacterial infection. CKC_05770 interacted with APX6 and APX7 in vivo assays but did not suppress ROS, HR or exhibited a peroxidase activity. Based on our results, we propose that interacting with APX proteins might not be sufficient to suppress these reactions. Further, our results suggest that the suppression of the ROS burst might not be linked to the interaction with APX6, but to the peroxidase function determined for the CLas protein.

Seven tomato APX genes have been identified and classified in three subgroups: cytoplasmic, chloroplastic and peroxisomal⁴⁷. Our tests demonstrated that CKC_05770 interacted in vivo with the chloroplastic APX6 and APX7 but not the cytoplasmic APX1 proteins. Furthermore, based on the BiFC results, the interaction occurred in the cell cytoplasm. APX6 and APX7 encode the thylakoid and stromal APX proteins, respectively. However, in *S. lycopersicum*, the stromal APX is targeted to chloroplast stroma and mitochondrial matrix^{48,49}. Therefore, this interaction could indeed play a significant role in the ROS responses against *Liberibacter* pathogens which are phloem restricted pathogens.

In conclusion, based on our results, LsoB non-traditional secreted proteins can be secreted and some of these proteins might play a role in plant defense mechanisms. We determined that LsoB prophages do not replicate when the pathogen is associated with psyllids or tomato plants in laboratory conditions. Finally, while we did not find any evidence that the non-classical secretory LsoB proteins CKC_05770 or CKC_00930 can induce or

reduce HR or ROS responses in the performed bioassays, and that while CKC_05770 did not have a peroxidase function, it interacted with the APX6 and APX7 in vivo and therefore could have a role in the defenses against LsoB. The role of CKC_00930, if any, remains unknown. Overall, our results highlight that *Liberibacter* pathogens use different mechanisms to suppress plant defenses. Although the effectors and their interactors might be conserved, the role of these proteins and their function for plant defenses might be different.

Materials and methods

Bioinformatic analyses

LsoA (LsoNZ, ASM96808v1), LsoB (CLso-ZC1, ASM18366v1), LsoC (FIN114, ASM198367v1), LsoD (ISR100, ASM291824v2), CLas (psy62, ASM2376v2) and *L. crescens* (BT-0, ASM154330v1) predicted proteins were analyzed to identify non-classical secreted proteins using SecretomeP2.0²⁹ and SignalP6.0⁵⁰. A protein was considered a non-classical secreted protein candidate if it had a SignalP prediction as NO_SP, meaning that it was not predicted to be secreted by any of the classical bacterial secretion systems by SignalP, and a SecretomeP score SecP > 0.7. While a SecP score > 0.5 can be used to identify non-classical secreted proteins, we applied a more stringent cut-off in this study.

BLASTP and BLASTN (<https://blast.ncbi.nlm.nih.gov/Blast.cgi>) analyses were performed to identify protein homologs to CKC_05770 and CKC_00930 (Accession numbers: ADR52899.1 and ADR51937.1). The identified homolog sequences were downloaded and a phylogenetic analysis was performed with the “one click” mode using phylogeny.fr⁵¹. Briefly, the sequences were aligned using MUSCLE⁵² and the alignment was curated with Gblocks⁵³. Finally, PhyML was used to build the tree⁵⁴ and TreeDyn to draw it⁵⁵. All the sequence accession numbers are provided in the text. The tomato ascorbate peroxidase family has been previously studied in detail⁴⁷ and information available in NCBI such as sequence for primer design was retrieved as needed. Interproscan was used to identify domains.

Plants

Nicotiana benthamiana and *Solanum lycopersicum* L. ‘MoneyMaker’ (Thompson & Morgan Inc., Jackson, NJ) were grown from seeds in Jolly Gardener ProLine C25 soil. Miracle-Gro Water-Soluble Tomato Plant Food following the label rate (18-18-21 NPK; Scotts Miracle-Gro Company, Marysville, OH) was used as fertilizer.

RNA and DNA extraction, and gene expression analysis

DNA and RNA were purified from LsoB-infected psyllids and tomato plants. DNA purifications were performed as previously described⁵⁶. RNA was purified using a RNeasy Mini kit (Qiagen, Hilden, Germany) followed by DNase treatment with Turbo DNase (Ambion, Invitrogen, CA). Complementary DNA was synthesized using Verso cDNA Synthesis kit (Thermo Fisher Scientific, Waltham, MA) kit.

For cloning, Lso and tomato genes were amplified from these cDNAs using the Phusion High-Fidelity DNA Polymerase (New England Biolabs, Ipswich, MA). For sequence validation, amplicons were cloned into pGEM-T Easy (Promega, Madison, WI), transformed into *Escherichia coli* One Shot TOP10 (Thermo Fisher Scientific) competent cells and sequenced. All primers are reported in Table S1.

For gene expression analyses, RT-qPCR was performed using SensiFAST SYBR Hi-ROX Kit (Bioline, Taunton, MA) following the manufacturer’s recommendations. For each reaction, 5 ng of cDNA was combined with 250 nM of each primer and 1X of SYBR Green Master Mix. The final volume was adjusted to 10 µL using nuclease-free water. The RT-qPCR program was 95 °C for 2 min followed by 40 cycles at 95 °C for 5 s and 60 °C for 30 s. RT-qPCR assays were performed using a QuantStudio™ 6 Flex Real-Time PCR System (Applied Biosystems). Each sample was tested in triplicates with a negative control in each run and three independent replicates. The relative expression of the candidate genes was estimated with the $\Delta\Delta C_T$ method using RecA as the reference gene⁵⁷. For gene quantification, qPCRs were performed similarly using DNA as template using RecA as the reference.

Protein secretion validation

To validate if the candidate proteins were secreted, the full-length sequence was cloned in frame with the gene *PhoA* into the pJDT-SDM1. The construct was transformed into One Shot TOP10 competent cells. Then, the bacteria were grown on Lysogeny Broth agar supplemented with ampicillin at 100 µg/mL, chromogenic substrate 5-bromo-4-chloro-3-indolyl phosphate (5-BCIP) at 90 µg/mL, and 75 mM Na₂PO₄ to block the endogenous phosphatase activity. We also evaluated the secretion by culturing the bacteria in liquid medium and filtering the media through a 0.2 µm filter before adding 5-BCIP. Detailed procedures are described in^{26,58}.

Yeast two hybrid (Y2H) assays

Amplified PCR amplicons were cloned into pDONR-207 vector (Thermo Fisher Scientific) using Gateway BP Clonase II (Thermo Fisher Scientific) according to the manufacturer’s directions. The resulting clones were used to subclone into the destination vectors for further work. For the Y2H assays, the sequence encoding CKC_05770 and CKC_00930 and well as the N-terminal portion of CKC_05770, hereafter named CKC_05770N, were cloned into the pDEST-GBKT7 vector as bait and transformed into Y2H Gold yeast (Takara, San Jose, CA). Full-length *S. lycopersicum* APX1, APX6 and APX7 coding sequences were cloned separately into the pDEST-GADT7 vector as prey and transformed into Y187 yeast (Takara).

Yeast carrying specific combinations of prey and bait constructs were mated and plated on the SD-Leu-Trp (double drop-out, DDO) medium. Yeast clones with paired constructs that grew on the DDO medium were resuspended in 100 µL of sterile water then 10 µL droplets of the culture dilutions were transferred onto plates containing DDO, SD-Leu-Trp-His- (triple drop-out, TDO) and on SD-Leu-Trp-His-Adenine (quadruple drop-out, QDO) media.

Bi-molecular fluorescence complementation (BiFC)

The full-length sequences of LsoB CKC_05770 and CKC_00930, and *S. lycopersicum* APX6 and APX7 genes were cloned into pEarleyGate-201-YN (pEG201-YN) vector (Lso genes), and pEarleyGate202-YC (pEG202-YC) vector (tomato genes). The cloning constructs were introduced separately into *Agrobacterium tumefaciens* strain LBA4404 by electroporation.

Agrobacterium tumefaciens culture and plant infiltration were performed as in Kan, et al.⁵⁹. Briefly, *A. tumefaciens* cultures were pelleted and resuspended in freshly prepared infiltration buffer (10 mM MgCl₂, 10 mM morpholineethanesulfonic acid (MES), and 200 μ M acetosyringone (AS)) at a final OD₆₀₀ of 0.7. The bacteria with the BiFC constructs were co-infiltration at v/v ratio = 1:1 into the leaves of 4-week-old *N. benthamiana* plants using a needleless syringe. The plants were maintained at room temperature. After 48 to 80 h following infiltration, the infiltrated leaves were observed using a fluorescent microscope (Axio Imager A1 microscope, Carl Zeiss Microscopy, White Plains, NY, USA) with a FITC (488 nm, green) filter for YFP signal.

Pull-down assay

In vitro pull-down assays were conducted to validate the interactions of CKC_05770 with APX7. CKC_05770 was cloned into the pFN2A (GST) (Promega) vector using SgfI and PmeI restriction enzymes. Also, the pFN2A (GST) vector was modified to remove barnase and express GST only; this construct was used as control. Tomato APX7 were cloned into pET101 vector (Thermo Fisher Scientific). The resulting constructs were transformed into *E. coli* BL21, and the transformed cells were cultured overnight. The next day, one subculture from each transformation was prepared, and induced with 0.5 mM IPTG. The GST pull-down assay was conducted in accordance with the manufacturer's instructions using the Pierce GST Protein Interaction Pull-Down Kit (Pierce Biotechnology, Rockford, IL). Briefly, the cells harboring the pFN2A (bait) and the pET101 (prey) vectors were lysed using the Pull-Down Lysis Buffer. The bait proteins were immobilized to glutathione affinity resin columns at 4 °C. The prey samples were added to the bait columns and incubated at 4 °C for one hour; the columns were then washed several times with the wash solution. The bait and prey bounded protein were then mixed with 4X LSD sample buffer and loaded onto each lane of 4–12% Bis-Tris NuPage gel (Invitrogen) and separated by SDS-PAGE. The proteins were transferred onto an Immobilon-P PVDF membrane (Millipore-Sigma, Burlington, MA) using a normal blotting procedure. The Ponceau S staining was used to visualize the loading of proteins. The membrane was subsequently blocked using 5% dry milk in TBST buffer, followed by incubation with the primary antibodies, rabbit anti-GST (Invitrogen, A-5800) or mouse anti-His (Thermo Fisher Scientific) at 4 °C overnight. The blots were washed and then probed with HRP-conjugated secondary antibodies for 1 h at room temperature. The bound antibody was detected with the SuperSignal West Pico substrate (Invitrogen) and imaged on an iBright 1500 imaging system (Thermo Fisher Scientific).

Agrobacterium tumefaciens-mediated transient expression, cell death and reactive oxygen species responses

Agrobacterium tumefaciens grown as described above carrying CKC_05770 or CKC_00930 cloned into the pEarleyGate 101 (pEG101) plasmid were infiltrated singly or in co-infiltration with *A. tumefaciens* carrying Pr^{D1416V} as described in Levy et al.²⁶ into five-week-old *N. benthamiana* leaves. The plants were maintained on light shelves at room temperature (approximately 24°C). Cell death was scored on a scale of 0 (no reaction) to 10 (cell death in all the infiltrated area) for each infiltration. The co-infiltration of Pr^{D1416V} with AvrPto1 and with an empty pEG101 vector were used as control. The experiments were performed at least three times. Each time, a minimum of 3 leaves per plant, and between 3 and 5 plants were infiltrated. Similar assays were performed co-infiltrating *A. tumefaciens* carrying CKC_05770 or CKC_00930 cloned into the pEG101 plasmid with *A. tumefaciens* carrying BAX. Co-infiltration of BAX with an empty pEG101 was used as control.

Agroinfiltrated leaves were also used to evaluate ROS responses following the procedure described by Bisceglia, Gravino and Savatin⁶⁰. To do so, 24 h after single infiltration, leaf disks were excised from agroinfiltrated zones and placed in 96-well plates. The disks were incubated overnight in water. The next day, the water was removed and replaced with 100 μ L of an assay solution (17 mM luminol and 1 μ M horseradish peroxidase). The luminescence was measured for 5 cycles using an Infinite 200 PRO NanoQuant plate reader (Tecan, Männedorf, Switzerland), then 1 μ M flg22 was added to each well and the luminescence was measured for 35 additional cycles. The experiment was repeated three times, each repetition included at least four plants. There were three technical replicates each time (leaf disks). The luminescence produced by the leaf disks agroinfiltrated with the candidates and with the empty vector was compared.

Additionally, to evaluate the subcellular localization of the proteins, *N. benthamiana* infiltrated leaves were observed using the fluorescent microscope as previously described and cells expressing CKC_05770 were also observed with an Olympus FV3000 laser scanning confocal system mounted to an Olympus IX83 (Olympus America, Center Valley, PA, USA). YFP fluorescence was excited at a wavelength of 512 nm, with emission detected within the range of 525 nm to 600 nm. The nucleus was stained using DAPI, excited at 358 nm, and detected at 461 nm. The autofluorescence from chloroplasts was excited at 695 nm, with emission measured between 715 nm and 740 nm. The images were combined using Fiji ImageJ software⁶¹. Western blot analyses were performed from proteins purified from infiltrated leaves using the HA-tag to detect the expression of the CKC_05770 and CKC_00930 proteins two days after the agroinfiltration (Fig. S1).

Peroxidase assay

CKC_05770 was cloned into Champion pET101 (Thermo Fisher Scientific) vector by directional TOPO cloning. *Escherichia coli* BL21 cells were transformed with the construct and grown overnight at 37 °C. The next day, four subcultures were made, and two of them were induced with 0.1 mM IPTG. Two hours after IPTG induction, one induced and one non-induced culture were treated with 3% H₂O₂. From the original subculture, we had

four treatments: 05770, 05770 + IPTG, 5770 + H₂O₂, and 5770 + IPTG + H₂O₂. For each culture, the OD₆₀₀ was measured every 60 min for five hours. The experiment was repeated three times. The expression of CKC_05770 in *E. coli* was verified by Western blot using anti His Tag antibodies (Thermo Fisher Scientific).

Data analysis

R (<https://www.r-project.org/>) and GraphPad Prism (GraphPad Software, San Diego, CA, USA) were used for data analysis. Student's T-tests were performed for gene expression and copy number analyses between infected plants and infected psyllids. The results from the HR assays and the ROS assays were analyzed by Kruskal-Wallis followed by pairwise comparisons using Wilcoxon rank sum test with continuity correction to identify significant differences.

Data availability

Data is provided within the manuscript or supplementary information files.

Received: 18 April 2024; Accepted: 6 March 2025

Published online: 28 March 2025

References

- Wen, A. et al. Detection, distribution, and genetic variability of '*Candidatus liberibacter*' species associated with zebra complex disease of potato in North America. *Plant. Dis.* **93**, 1102–1115. <https://doi.org/10.1094/PDIS-93-11-1102> (2009).
- Munyaneza, J. E. et al. First report of *Candidatus liberibacter solanacearum* associated with psyllid-affected carrots in Europe. *Plant. Dis.* **94**, 639–639. <https://doi.org/10.1094/PDIS-94-5-0639A> (2010).
- Teresani, G. R. et al. Association of '*Candidatus liberibacter solanacearum*' with a vegetative disorder of celery in Spain and development of a real-time PCR method for its detection. *Phytopathology* **104**, 804–811. <https://doi.org/10.1094/phyto-07-13-0182-r> (2014).
- Nelson, W. R. et al. A new haplotype of *Candidatus liberibacter solanacearum* identified in the mediterranean region. *Eur. J. Plant Pathol.* **135**, 633–639 (2013).
- Tahzima, R. et al. First report of '*Candidatus liberibacter solanacearum*' on Carrot in Africa. *Plant. Dis.* **98**, 1426–1426. <https://doi.org/10.1094/pdis-05-14-0509-pdn> (2014).
- Haapalainen, M. et al. A novel haplotype of '*Candidatus liberibacter solanacearum*' found in Apiaceae and Polygonaceae family plants. *Eur. J. Plant. Pathol.* **156**, 413–423. <https://doi.org/10.1007/s10658-019-01890-0> (2020).
- Haapalainen, M. L. et al. Genetic variation of '*Candidatus liberibacter solanacearum*' haplotype C and identification of a novel haplotype from *Trioxa urticae* and stinging nettle. *Phytopathology* **108**, 925–934 (2018).
- Munyaneza, J., Crosslin, J. A., Upton, J. Association of *Bactericera cockerelli* (Homoptera: Psyllidae) with zebra chip, a new potato disease in Southwestern United States and Mexico. *J. Econ. Entomol.* **100**, 656–663 (2007).
- Munyaneza, J. E., Goolsby, J. A., Crosslin, J. M. & Upton, J. E. Further evidence that zebra chip potato disease in the lower Rio Grande Valley of Texas is associated with *Bactericera cockerelli*. (2007).
- Mustafa, T. et al. Use of electrical penetration graph technology to examine transmission of '*Candidatus liberibacter solanacearum*' to potato by three haplotypes of potato psyllid (*Bactericera cockerelli*; hemiptera: Trioziidae). *PLoS One*. **10**, e0138946 (2015).
- Teresani, G. R. et al. Association of '*Candidatus liberibacter solanacearum*' with a vegetative disorder of celery in Spain and development of a real-time PCR method for its detection. *Phytopathology* **104**, 804–811 (2014).
- Mawassi, M. et al. *Candidatus liberibacter solanacearum*'s tightly associated with Carrot yellows symptoms in Israel and transmitted by the prevalent psyllid vector *bactericera trigonica*. *Phytopathology* **108**, 1056–1066 (2018).
- Munyaneza, J. et al. First report of *Candidatus liberibacter solanacearum* associated with psyllid-affected carrots in Europe. *Plant. Dis.* **94**, 639 (2010).
- Tahzima, R. et al. First report of '*Candidatus liberibacter solanacearum*' on Carrot in Africa. *Plant. Dis.* **98**, 1426 (2014).
- Wang, N. et al. The *Candidatus Liberibacter*-host interface: insights into pathogenesis mechanisms and disease control. *Annu. Rev. Phytopathol.* **55**, 451–482. <https://doi.org/10.1146/annurev-phyto-080516-035513> (2017).
- Deslandes, L. & Rivas, S. Catch me if you can: bacterial effectors and plant targets. *Trends Plant Sci.* **17**, 644–655. <https://doi.org/10.1016/j.tplants.2012.06.011> (2012).
- Duan, Y. et al. Complete genome sequence of citrus Huanglongbing bacterium, '*Candidatus liberibacter Asiaticus*' obtained through metagenomics. *Mol. Plant. Microbe Interact.* **22**, 1011–1020. <https://doi.org/10.1094/mpmi-22-8-1011> (2009).
- Lin, H. et al. The complete genome sequence of '*Candidatus liberibacter solanacearum*', the bacterium associated with potato zebra chip disease. *PLoS One*. **6**, e19135 (2011).
- Clark, K. et al. An effector from the Huanglongbing-associated pathogen targets citrus proteases. *Nat. Commun.* **9**, 1718–1718. <https://doi.org/10.1038/s41467-018-04140-9> (2018).
- Jain, M., Munoz-Bodnar, A., Zhang, S. & Gabriel, D. W. A secreted '*Candidatus liberibacter Asiaticus*' Peroxiredoxin simultaneously suppresses both localized and systemic innate immune responses in planta. *Mol. Plant Microbe Interact.* **31**, 1312–1322. <https://doi.org/10.1094/MPMI-03-18-0068-R> (2018).
- Pitino, M., Armstrong, C. M., Cano, L. M. & Duan, Y. Transient expression of *Candidatus liberibacter Asiaticus* effector induces cell death in *Nicotiana benthamiana*. *Front. Plant. Sc.* **7**, 982–982. <https://doi.org/10.3389/fpls.2016.00982> (2016).
- Prasad, S., Xu, J., Zhang, Y. & Wang, N. SEC-translocon dependent extracytoplasmic proteins of *Candidatus liberibacter Asiaticus*. *Front. Microbiol.* **7**, 1989–1989. <https://doi.org/10.3389/fmicb.2016.01989> (2016).
- Oh, J., Levy, J. G., Kan, C. C., Ibanez-Carrasco, F. & Tamborindeguy, C. CLIBASIA_00460 disrupts hypersensitive response and interacts with citrus Rad23 proteins. *Int. J. Mol. Sci.* **23**, 7846 (2022).
- Pang, Z. et al. Citrus CsACD2 is a target of *Candidatus liberibacter Asiaticus* in Huanglongbing disease. *Plant Physiol.* **184**, 792–805. <https://doi.org/10.1104/pp.20.00348> (2020).
- Reyes Caldas, P. A. et al. Effectors from a bacterial vector-borne pathogen exhibit diverse subcellular localization, expression profiles, and manipulation of plant defense. *Mol. Plant Microbe Interact.* **35**, 1067–1080. <https://doi.org/10.1094/mpmi-05-22-0114-r> (2022).
- Levy, J. G. et al. Lso-HPE1, an effector of '*Candidatus liberibacter solanacearum*', can repress plant immune response. *Phytopathology* **110**, 648–655 (2020).
- Ravindran, A. et al. Characterization of the serralsin-like gene of '*Ca. Liberibacter solanacearum*' associated with potato zebra chip disease. *Phytopathology* **108**, 327–335 (2017).
- Levy, J. G. et al. A '*Candidatus liberibacter solanacearum*' haplotype B-specific family of candidate bacterial effectors. *Phytopathology* **113**, 1708–1715 (2023).
- Bendtsen, J. D., Kiemer, L., Fausbøll, A. & Brunak, S. Non-classical protein secretion in bacteria. *BMC Microbiol.* **5**, 58. <https://doi.org/10.1186/1471-2180-5-58> (2005).

30. Jain, M., Fleites, L. A. & Gabriel, D. W. Prophage-encoded peroxidase in '*Candidatus liberibacter Asiaticus*' is a secreted effector that suppresses plant defenses. *Mol. Plant-Microbe Interactions*. **28**, 1330–1337. <https://doi.org/10.1094/mpmi-07-15-0145-r> (2015).
31. Du, P. et al. *Candidatus liberibacter Asiaticus* secretes nonclassically secreted proteins that suppress host hypersensitive cell death and induce expression of plant pathogenesis-related proteins. *Appl. Environ. Microbiol.* **87** <https://doi.org/10.1128/aem.00019-21> (2021).
32. Harrison, K. et al. Differences in zebra chip severity between '*Candidatus liberibacter solanacearum*' haplotypes in Texas. *Am. J. Potato Res.* **96**, 86–93 (2019).
33. Levy, J. G. et al. Evaluation of the effect of *Candidatus liberibacter solanacearum* haplotypes in tobacco infection. *Agronomy* **13**, 569 (2023).
34. Mendoza Herrera, A. et al. Infection by '*Candidatus liberibacter solanacearum*' haplotypes A and B in *Solanum lycopersicum* 'moneymaker'. *Plant. Dis.* **102**, 2009–2015. <https://doi.org/10.1094/PDIS-12-17-1982-RE> (2018).
35. Zhang, S. et al. Ca. *Liberibacter asiaticus* carries an excision plasmid prophage and a chromosomally integrated prophage that becomes lytic in plant infections. *Mol. Plant-Microbe Interactions*. **24**, 458–468. <https://doi.org/10.1094/mpmi-11-10-0256> (2011).
36. Lacomme, C. & Santa Cruz, S. Bax-induced cell death in tobacco is similar to the hypersensitive response. *Proc. Natl. Acad. Sci. U.S.A.* **96**, 7956–7961 (1999).
37. Du, J. et al. A prophage-encoded effector from *Candidatus liberibacter Asiaticus* targets ASCORBATE PEROXIDASE6 in citrus to facilitate bacterial infection. *Mol. Plant. Pathol.* **24**, 302–316. <https://doi.org/10.1111/mpp.13296> (2023).
38. Ding, F., Allen, V., Luo, W., Zhang, S. & Duan, Y. Molecular mechanisms underlying heat or Tetracycline treatments for citrus HLB control. *Hortic. Res.* **5**, 30. <https://doi.org/10.1038/s41438-018-0038-x> (2018).
39. Jain, M., Fleites, L. A. & Gabriel, D. W. A small Wolbachia protein directly represses phage lytic cycle genes in *Candidatus liberibacter Asiaticus* within psyllids. *mSphere* **2** <https://doi.org/10.1128/mSphereDirect.00171-17> (2017).
40. Fleites, L. J., Zhang, M., Gabriel, D. S. *Candidatus liberibacter Asiaticus* prophage late genes May limit host range and culturability. *Appl. Environ. Microbiol.* **80**, 6023–6030. <https://doi.org/10.1128/AEM.01958-14> (2014).
41. Lukan, T. & Coll, A. Intertwined roles of reactive oxygen species and Salicylic acid Signaling are crucial for the plant response to biotic stress. *Int. J. Mol. Sci.* **23** <https://doi.org/10.3390/ijms23105568> (2022).
42. Maffei, M. E., Mithöfer, A. & Boland, W. Before gene expression: early events in plant-insect interaction. *Trends Plant. Sci.* **12**, 310–316. <https://doi.org/10.1016/j.tplants.2007.06.001> (2007).
43. Maruta, T., Sawa, Y., Shigeoka, S. & Ishikawa, T. Diversity and evolution of ascorbate peroxidase functions in chloroplasts: more than just a classical antioxidant enzyme? *Plant. Cell. Physiol.* **57**, 1377–1386. <https://doi.org/10.1093/pcp/pcv203> (2016).
44. Saxena, S. C. et al. Ectopic overexpression of cytosolic ascorbate peroxidase gene (Apx1) improves salinity stress tolerance in *Brassica juncea* by strengthening antioxidative defense mechanism. *Acta Physiol. Plant.* **42**, 45. <https://doi.org/10.1007/s11738-020-3032-5> (2020).
45. Durner, J. & Klessig, D. F. Inhibition of ascorbate peroxidase by Salicylic acid and 2,6-dichloroisonicotinic acid, two inducers of plant defense responses. *Proc. Natl. Acad. Sci. U.S.A.* **92**, 11312–11316. <https://doi.org/10.1073/pnas.92.24.11312> (1995).
46. Wang, Y. et al. Overexpression of cytosolic ascorbate peroxidase in tomato confers tolerance to chilling and salt stress. *J. Am. Soc. Hortic. Sci.* **130**, 167–173. <https://doi.org/10.21273/jashs.130.2.167> (2005).
47. Najami, N. et al. Ascorbate peroxidase gene family in tomato: its identification and characterization. *Mol. Genet. Genomics*. **279**, 171–182. <https://doi.org/10.1007/s00438-007-0305-2> (2008).
48. Mittova, V. et al. Comparison of mitochondrial ascorbate peroxidase in the cultivated tomato, *Lycopersicon esculentum*, and its wild, salt-tolerant relative, *L. pennellii*—a role for matrix isoforms in protection against oxidative damage. *Plant. Cell. Environ.* **27**, 237–250. <https://doi.org/10.1046/j.1365-3040.2004.01150.x> (2004).
49. Jardim-Messeder, D., Zamocky, M., Sachetto-Martins, G. & Margis-Pinheiro, M. Chloroplastic ascorbate peroxidases targeted to stroma or thylakoid membrane: the chicken or egg dilemma. *FEBS Lett.* **596**, 2989–3004. <https://doi.org/10.1002/1873-3468.14438> (2022).
50. Teufel, F. et al. SignalP 6.0 predicts all five types of signal peptides using protein Language models. *Nat. Biotechnol.* <https://doi.org/10.1038/s41587-021-01156-3> (2022).
51. Dereeper, A. et al. Phylogeny.fr: robust phylogenetic analysis for the non-specialist. *Nucleic Acids Res.* **36**, W465–469. <https://doi.org/10.1093/nar/gkn180> (2008).
52. Edgar, R. C. MUSCLE: multiple sequence alignment with high accuracy and high throughput. *Nucleic Acids Res.* **32**, 1792–1797. <https://doi.org/10.1093/nar/gkh340> (2004).
53. Castresana, J. Selection of conserved blocks from multiple alignments for their use in phylogenetic analysis. *Mol. Biol. Evol.* **17**, 540–552. <https://doi.org/10.1093/oxfordjournals.molbev.a026334> (2000).
54. Guindon, S. & Gascuel, O. A simple, fast, and accurate algorithm to estimate large phylogenies by maximum likelihood. *Syst. Biol.* **52**, 696–704. <https://doi.org/10.1080/10635150390235520> (2003).
55. Chevenet, F., Brun, C., Bañuls, A. L., Jacq, B. & Christen, R. TreeDyn: towards dynamic graphics and annotations for analyses of trees. *BMC Bioinform.* **7**, 439. <https://doi.org/10.1186/1471-2105-7-439> (2006).
56. Levy, J., Ravindran, A., Gross, D., Tamborindéguy, C. & Pierson, E. Translocation of '*Candidatus liberibacter solanacearum*', the zebra chip pathogen, in potato and tomato. *Phytopathology* **101**, 1285–1291 (2011).
57. Ibanez, F., Levy, J. & Tamborindéguy, C. Transcriptome analysis of *Candidatus liberibacter solanacearum* in its psyllid vector, *Bactericera cockerelli*. *PLoS ONE*. **9**, e100955 (2014).
58. Ammerman, N., Sayeedur Rahman, M. & Azad, A. F. Characterization of sec-translocon-dependent extracytoplasmic proteins of *Rickettsia typhi*. *J. Bacteriol.* **190**, 6234–6242 (2008).
59. Kan, C. C. et al. HPE1, an effector from zebra chip pathogen interacts with tomato proteins and perturbs ubiquitinated protein accumulation. *Int. J. Mol. Sci.* **22**, 9003 (2021).
60. Bisceglia, N. G., Gravino, M. & Savatin, D. V. Luminol-based assay for detection of immunity elicitor-induced hydrogen peroxide production in *Arabidopsis thaliana* leaves. *Bio-protocol* **5**, e1685. <https://doi.org/10.21769/BioProtoc.1685> (2015).
61. Schindelin, J. et al. Fiji: an open-source platform for biological-image analysis. *Nat. Methods*. **9**, 676–682. <https://doi.org/10.1038/nmeth.2019> (2012).

Acknowledgements

The authors thank the Agriculture Women Excited to Share Opinions, Mentoring and Experiences (AWESOME) faculty group of the College of Agriculture and Life Sciences at Texas A&M University for assistance with editing the manuscript. Junepyo Oh received the Herb Dean'40 Endowed scholarship from the Department of Entomology at Texas A&M University. Support was provided by Texas A&M University and Texas A&M AgriLife Research through the Controlling Exotic and Invasive Insect-Transmitted Pathogens; Texas A&M University Hatch Projects to JGL TEX0-9934-0 (accession number 7002235) and to CT TEX0- 9381-2 (accession number 7005355).

Author contributions

Conceptualization, J.G.L. and C.T.; methodology, A.P., J.G.L., M.A.M.H., J.O., and B.D.S.; formal analysis J.G.L., A.P., J.O. and C.T.; writing, A.P., J.G.L. and C.T.; supervision J.G.L., C.T.; funding acquisition, J.G.L., and C.T. All authors reviewed the manuscript.

Funding

Support was provided by Texas A&M University and Texas A&M AgriLife Research through the Controlling Exotic and Invasive Insect-Transmitted Pathogens; Texas A&M University Hatch Projects to JGL TEX0-9934-0 (accession number 7002235) and to CT TEX0-9381-2 (accession number 7005355).

Declarations

Competing interests

The authors declare no competing interests.

Additional information

Supplementary Information The online version contains supplementary material available at <https://doi.org/10.1038/s41598-025-93367-w>.

Correspondence and requests for materials should be addressed to J.G.L. or C.T.

Reprints and permissions information is available at www.nature.com/reprints.

Publisher's note Springer Nature remains neutral with regard to jurisdictional claims in published maps and institutional affiliations.

Open Access This article is licensed under a Creative Commons Attribution-NonCommercial-NoDerivatives 4.0 International License, which permits any non-commercial use, sharing, distribution and reproduction in any medium or format, as long as you give appropriate credit to the original author(s) and the source, provide a link to the Creative Commons licence, and indicate if you modified the licensed material. You do not have permission under this licence to share adapted material derived from this article or parts of it. The images or other third party material in this article are included in the article's Creative Commons licence, unless indicated otherwise in a credit line to the material. If material is not included in the article's Creative Commons licence and your intended use is not permitted by statutory regulation or exceeds the permitted use, you will need to obtain permission directly from the copyright holder. To view a copy of this licence, visit <http://creativecommons.org/licenses/by-nc-nd/4.0/>.

© The Author(s) 2025